Essay Describing My Thesis Work

My thesis describes novel and interdisciplinary work, which invokes the well-established principles of organotin chemistry and addresses the problems that thwart the development of thrust areas of research such as multi-ferrocene and multi-porphyrin assemblies. In doing so, some interesting issues in organotin and organosilicon chemistry have also been addressed. They are elaborated in the following pages:

In recent years, multi-ferrocene assemblies, including polymeric derivatives, are receiving great interest in view of their promising applications. These include (a) redox-active materials for modification of electrodes (b) materials that can function as multi-electron redox systems and (c) biosensors. Among the synthetic approaches to prepare macromolecules containing ferrocenes, the most successful strategy has been the ring-opening polymerization of main group element-bridged [1] ferrocenophanes by thermal or anionic methods. In contrast to these linear polymers, syntheses of assemblies containing ferrocene units in a cyclic arrangement have been carried out by utilizing various strategies. However, all the synthetic strategies regularly suffer from most of the following drawbacks (a) multi-step synthesis, (b) low yield of the multi-ferrocene assemblies, (c) lack of crystallographic characterization of the final multi-ferrocene assembly and (d) non ideal electrochemical behavior of the resulting multi-ferrocene assemblies such as the multiple oxidation waves, decomposing waves and stripping peaks. In order to overcome these drawbacks we have adopted a radically different and simple synthetic strategy to assemble multi-ferrocene units on robust stannoxane supports. This is based on the principles of organotin chemistry. Thus, the reaction of n-butylstannonic acid, n-BuSn(O)OH with either ferrocenecarboxylic acid or ferrocenylacetic acid afforded the hexa-ferrocene assemblies [n-BuSn(O)OC(O)C$_5$H$_4$-Fe-C$_5$H$_5$]$_6$ and [n-BuSn(O)OC(O)CH$_2$C$_5$H$_4$-Fe-C$_5$H$_5$]$_6$ in nearly quantitative yields. Another important feature of this result is that it is a single-step synthesis from commercially available starting materials. The solid-state structure of these hexa-ferrocene assemblies as revealed by the single crystal X-ray crystallography shows a giant-wheel like arrangement of the six-ferrocene units on a central drum-like stannoxane core (Figure1). Also they are thermally and electrochemically robust as evident from their TGA and cyclic voltammetric studies. A single quasi-reversible oxidation wave indicative of the electrochemical equivalence of all the ferrocene units is observed for both the assemblies (Figure 2). Also the voltammogram is reproducible even after several continuous cycles and

the peak potential do not vary with the scan rates (10 mV to 200 mV S^{-1}). These indicate that the hexa-ferrocene assemblies do not decompose upon oxidation. The ^{119}Sn NMR studies in solution shows a single peak around -480 ppm characteristic of a drum like stannoxane core and reveals the retention of the structure in solution. Similarly by the choice of the organotin precursor and by altering the carboxylic acid ratio, other assemblies such as tetra-, di-, and mono-ferrocene derivatives are also obtained exclusively in near quantitative yields from commercially available reactants. Thus a 1:1 reaction of n-Bu$_2$SnO with ferrocene carboxylic or ferrocenylacetic acid gave the tetra-ferrocene assemblies namely {[n-Bu$_2$SnOC(O)C$_5$H$_4$-Fe-C$_5$H$_5$]$_2$O}$_2$ and {[n-Bu$_2$SnOC(O)CH$_2$C$_5$H$_4$-Fe-C$_5$H$_5$]$_2$O}$_2$. A similar reaction in a 1:2 ratio gave the di-ferrocene assemblies namely n-Bu$_2$Sn[OC(O)C$_5$H$_4$-Fe-C$_5$H$_5$]$_2$ and n-Bu$_2$Sn[OC(O)CH$_2$C$_5$H$_4$-Fe-C$_5$H$_5$]$_2$. The mono-ferrocene assemblies namely Ph$_3$SnOC(O)C$_5$H$_4$-Fe-C$_5$H$_5$ and Ph$_3$SnOC(O)CH$_2$C$_5$H$_4$-Fe-C$_5$H$_5$ have been prepared in a 1:2 reaction of Ph$_3$SnOSnPh$_3$ with the corresponding carboxylic acid. Thus, we have been able to modulate the extent of ferrocene incorporation by a variation of organotin precursor. No other synthetic procedure currently available, allows such easy manipulation.

Apart from the above interesting features most of these ferrocene assemblies form interesting supramolecular architectures in the solid state due to the presence of C-H---O interactions. Thus, in the case of the hexa-ferrocene assembly, [n-BuSn(O)OC(O)CH$_2$C$_5$H$_4$-Fe-C$_5$H$_5$]$_6$ a highly symmetric 2D-grid like structure is obtained (Figure 3). An exactly similar supramolecular array is also obtained in the case of hexa-mesityl assembly, [n-BuSn(O)OC(O)C$_6$H$_2$-2,4,6-Me$_3$]$_6$ (Figure 4). These are named as *Rangoli*[#] with tin drums (Figure 5). Interestingly in the case of the tetra-ferrocene assembly {[n-Bu$_2$SnOC(O)C$_5$H$_4$-Fe-C$_5$H$_5$]$_2$O}$_2$ a staircase like 1D-polymeric chain is obtained (Figure 6).

While these studies were in progress there was a great deal of interest in assembling functionalized dendrimers containing metalated sites in their periphery (multi-site coordination ligands), out of their promising application as homogeneous catalysts while retaining the advantages of heterogeneous systems. By considering the robustness of organostannoxane core in accommodating organometallic species in its periphery, we planned to anchor suitable ligating groups around the stannoxane core and to use such molecules as multi-site coordination ligands. An important starting material for such a study requires the assembly of a suitable carboxylic acid with potentially coordinating sites. We chose porphyrin carboxylic acid for this purpose out of various reasons such as rigidity, planar geometry, high stability, etc. By doing so, we have accomplished a dual advantage of getting multi-porphyrin and multi-metallaporphyrin assemblies apart from the multi-site

coordination ligands. Also from the literature it is known that multi-porphyrin assemblies are potentially important compounds because of their promising application in the field of molecular-scale electronics, optical devices, sensors, etc., and the development of this area is largely hampered by the lack of appropriate synthetic methods for their preparation. Conventional synthetic methods employ multi-step synthesis and extensive chromatographic purifications, which often result in very low yields of the multi-porphyrin arrays. In fact a successful synthetic strategy for multi-porphyrin assemblies should accomplish the following key requirements: a) free solubility b) easy separation c) reliable characterization and d) reasonable yield of the multi-porphyrin arrays. The individual porphyrinic character should also be retained after anchoring on the suitable support. Till now none of the synthetic strategies have incorporated all these features and my thesis throws light into these aspects and eradicates all these pitfalls using the organostannoxane route. Thus, the reaction of *n*-butylstannonic acid with 5-(4-carboxyphenyl)-10, 15, 20-tritolyl-21, 23-porphyrin (H_2TTPCOOH) in a 1:1 stoichiometry afforded the hexa-porphyrin assembly, [*n*-BuSn(O)OC(O)H_2TTP]$_6$ (Figure 7).   Remarkably this synthesis is a *one-step* procedure and the yields are nearly quantitative which is quite unprecedented for this family of compounds. Secondly there is no need for any chromatographic purification and quite importantly this is highly soluble in many common organic solvents. This surprising high solubility is due to the presence of lipophilic substituents on tin and due to the geometry of the drum-shaped organotin support which ensures the orthogonal arrangement of the porphyrin moieties with respect to each other. To prove its utility as multi-site coordination ligand as well as to prepare multi-metallaporphyrin arrays metalation studies have been carried out. This is accomplished in two ways a) by reacting the hexa-porphyrin assembly with metal precursors b) by preparing the metalated derivative of H_2TTPCOOH before hand and then reacting it with the organotin precursor to get the hexa-metalated porphyrin assembly. Using the first method a hexa-copper(II) porphyrin derivative, [*n*-BuSn(O)OC(O)CuTTP]$_6$ has been prepared and its formation portrays the integrity and cooperativity among the multi-porphyrin assembly and explains its robustness (Figure 8). By adopting the second method a hexa-palladium porphyrin assembly, [*n*-BuSn(O)OC(O)PdTTP]$_6$ has been prepared.   By changing the organotin precursor and by maintaining the porphyrin monocarboxylic acid ratio tetra-, di- and mono-porphyrin assemblies have also prepared exclusively.   All these compounds have been thoroughly and unambiguously characterized by MALDI-TOF mass spectroscopy as well as by multi-nuclear NMR. Further, detailed UV-Vis, Fluoresence, EPR and cyclic voltammetric studies reveal the retention of the individual porphyrinic character in the multi-

porphyrin assemblies and suggest the absence of any electronic interaction among the porphyrin rings and also with the core (Figure 9 & 10). Thus the organotin core acts as an ideal support and does not interfere with the porphyrinic character.

In view of the importance of fluorine containing organotin compounds as potential anti-cancer agents, this thesis also reports the reaction of a fluorine rich carboxylic acid 2,4,6-tris(trifluoromethyl)benzoic acid (R_fCOOH), with various organotin precursors. The results obtained are outlined below: Reaction of n-BuSn(O)OH with R_fCOOH in a 1:1 ratio gave a fluorine mammoth $[n$-BuSn(O)OC(O)(2,4,6-(CF$_3$)$_3$C$_6$H$_2$)]$_6$ which contains 54 fluorine atoms in its periphery (Figure 11). Also a 1:2 reaction of Ph$_3$SnOSnPh$_3$ with R_fCOOH leads for the first time, the formation of a Sn-C bond cleaved product [Ph$_2$Sn(OH)OC(O)(R$_f$)]$_2$ and not the usual product Ph$_3$SnOC(O)R$_f$ which is the scenario with more than fourty different aliphatic or aromatic carboxylic acids (Figure 12). Also in the solid-state [Ph$_2$Sn(OH)OC(O)(R$_f$)]$_2$ forms a 3D-supramolecular network out of the cumulative effect of C-H---O, C-F---π and C-H---F interactions. In an analogous similar reaction, $(n$-Bu)$_3$SnOSn(n-Bu)$_3$ affords, [n-Bu$_3$OC(O)R$_f$]$_n$ which crystallizes as a chiral helix (Figure 13). It is to be noted that such a chiral helix has been obtained from achiral building blocks. Such study has no precedence in organotin chemistry. Also it should be added here that the crystal system in which it has crystallized is not only a chiral space group but also a polar space group. This type of molecules has considerable applications in the area of piezoelectrics and non-linear optics.

In general and from the aforesaid discussions it is obvious that the reaction of mono organotin reagents with carboxylic acids offer only clusters and not simple products. Thus compounds such as monoorganotin tricarboxylate, RSn[OC(O)R']$_3$ are notoriously unstable and are considered as intermediates in the formation of ladders (open drum) and drums respectively. With the previous experience in organotin chemistry and by using 2-picolinic acid, first example of a monoorganotin tricarboxylate, n-BuSn(O$_2$CC$_5$H$_4$N)$_3$ has been obtained as a very stable product (Figure 14). The solid-state structure of this compound shows that the tin is hepta-coordinate with a CO$_4$N$_2$ donor set and the geometry is distorted pentagonal bipyramidal. Also due to the presence of C-H---O and π-π interactions a 3D-grid like supramolecular array is generated.

Apart from the work on Sn-O systems some interesting work on Si-O systems have also been carried out. Silanols, compounds containing Si-OH groups, are attracting the attention of number of researchers in view of their interesting structure and reactivity. Traditionally they find application as model compounds for silica surface and as precursors

for the synthesis of metallasiloxanes. Also in recent years new avenues for their application are emerging in the area of protease inhibitors, reagents in organic synthesis, etc. In view of these aspect my thesis report a series of novel N-bonded silicon dichlorides namely $RN(SiMe_3)(SiMeCl_2)$ [R = 2,6-$Me_2C_6H_3$, 2,4,6-$Me_3C_6H_2$, 2,6-i-$Pr_2C_6H_3$] and $RN(SiMe_3)(SiPhCl_2)$ [R = 2,6-$Me_2C_6H_3$] starting from 2,6- and 2,4,6-alkyl-substituted sterically hindered primary amines as starting materials. The structure of 2,6-i-$Pr_2C_6H_3N(SiMe_3)(SiMeCl_2)$ represents the first example of a N-bonded silicon dichloride that has been structurally characterized and also it is interesting from the crystallographic point of view as it has a positional disorder due to the presence of both Cl and CH_3 groups in the same molecule (Figure 15a). Controlled hydrolysis of these dichlorides afforded the corresponding N-bonded silanediols $RN(SiMe_3)(SiMe(OH)_2)$ [R = 2,6-$Me_2C_6H_3$, 2,4,6-$Me_3C_6H_2$, 2,6-i-$Pr_2C_6H_3$,] and $RN(SiMe_3)(SiPh(OH)_2)$ [R = 2,6-$Me_2C_6H_3$] in good yields (Figures 15b, 16a & 16b). The sterically hindered groups impart the necessary stability for the silanols by preventing their self-condensation process to form polymeric siloxanes. Also their solid-state structures show interesting correlations out of these remote steric groups on the aromatic ring. Accordingly, when the susbstituent is xylyl or mesityl a 1D-polymeric ribbon like structure is formed out of strong O-H---O interaction (Figures 17a & 17b). But when the substituent is isopropyl discrete hexameric clusters are formed instead of the expected polymeric structures (Figures 18). Thus, the increasing steric bulk decreases the realization of polymeric network and with this result, in principle it should be possible to modulate the type of solid-state structures formed by silanols.

Bis-silanetriols are a new class of compounds which contain two $-Si(OH)_3$ groups. As a matter of fact, stabilizing molecules with one $-Si(OH)_3$ group itself is difficult and requires an exact balance of steric and electronic factors. Because of this, these compounds have not been known for a very long time. This thesis reports the first example of a bis-N-bonded silanetriol, $[(OH)_3SiN(SiMe_3)]_2C_6(2,3,5,6-Me_4)$ prepared from 2,3,5,6-tetramethyl-1,4-phenylenediamine via the corresponding bis-N-bonded silicon trichloride, $[(Cl)_3SiN(SiMe_3)]_2C_6(2,3,5,6-Me_4)$. These compounds have been characterized by mass, multi-nuclear and IR spectral techniques. Energy minimized structure of the bis-N-bonded silanetriol as obtained from semi-empirical AM1 calculation is also reported (Figure 19).
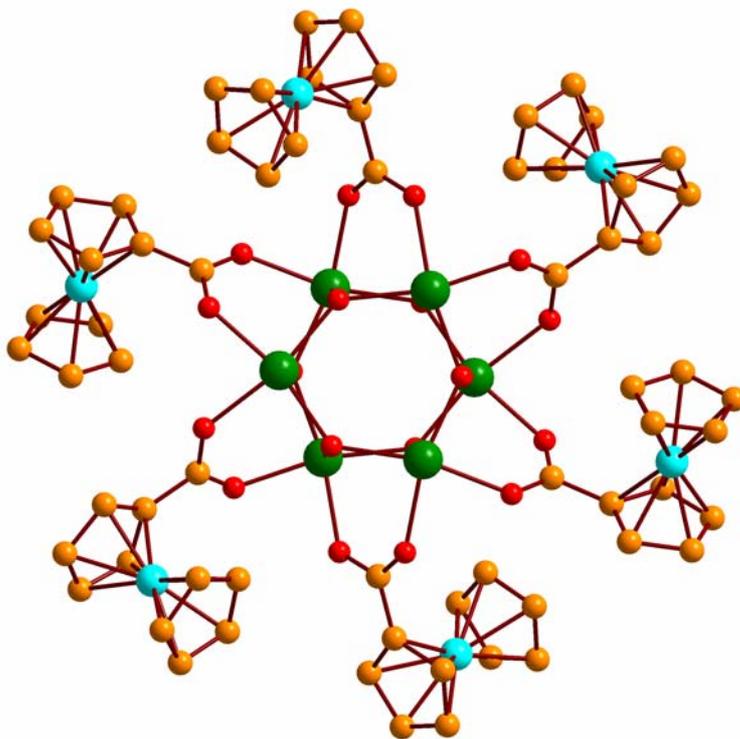
Figure 1. X-ray crystal structure of the hexa-ferrocene assembly

[*n*-BuSn(O)OC(O)C$_5$H$_4$-Fe-C$_5$H$_5$]$_6$
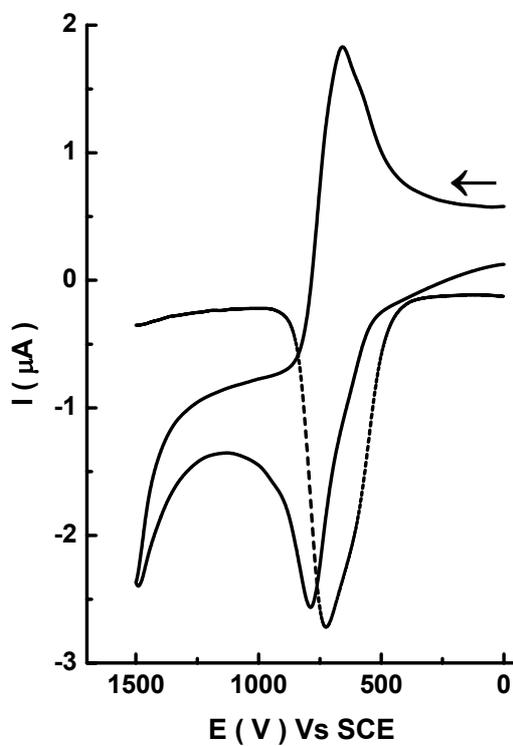
Figure 2. Cyclic (——) and differential pulse (----) voltammogram of

[*n*-BuSn(O)OC(O)C$_5$H$_4$-Fe-C$_5$H$_5$]$_6$
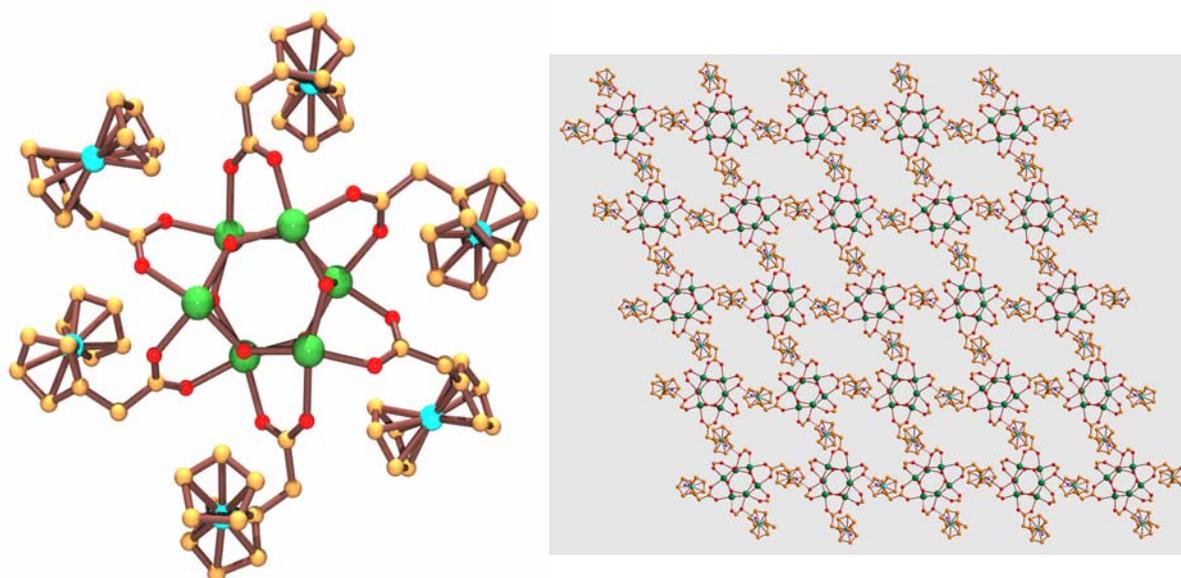
**Figure 3. Molecular and 2D-grid like supramolecular (out of C-H---O interactions) structure of the hexa-ferrocene assembly [n-BuSn(O)OC(O)CH$_2$C$_5$H$_4$-Fe-C$_5$H$_5$]$_6$**
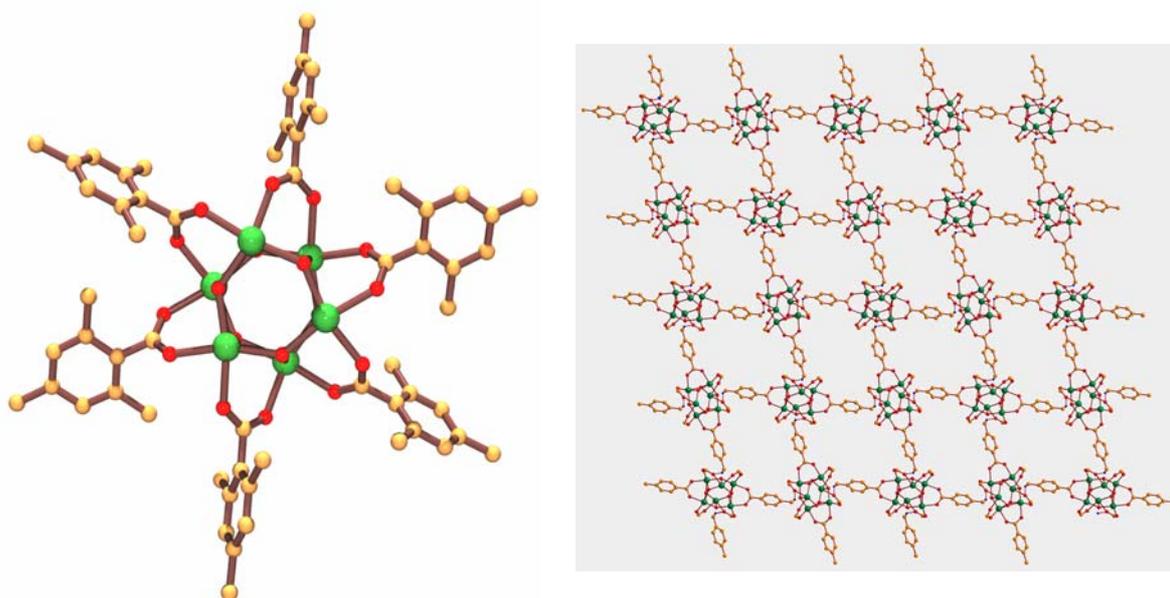
Figure 4. Molecular and 2D-grid like supramolecular (out of C-H---O interactions) structure of the hexa-mesityl derivative, [n-BuSn(O)OC(O)C$_6$H$_2$-2,4,6-Me$_3$]$_6$
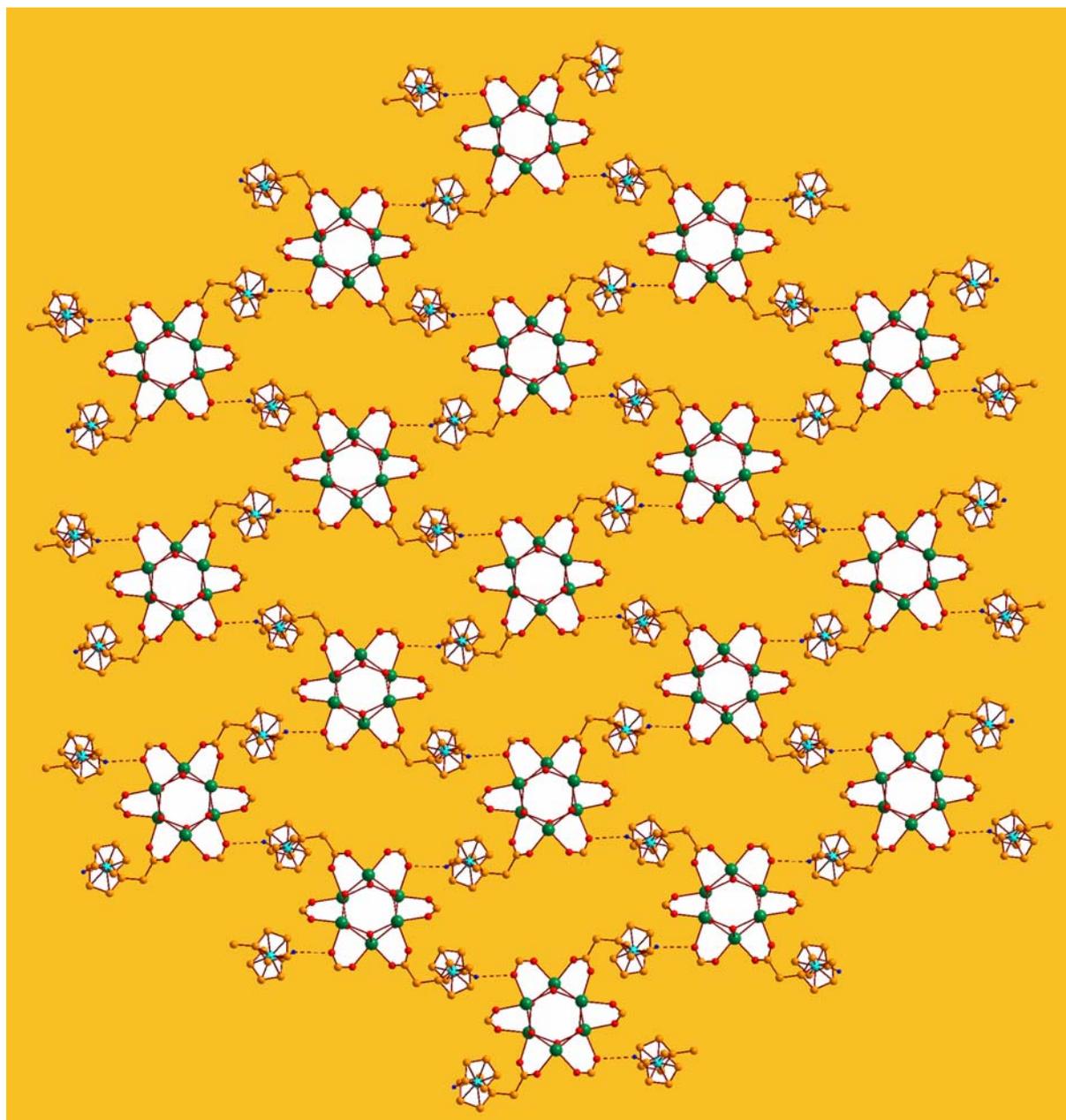
Figure 5. View showing the *Rangoli* [#] like arrangement of the 2D-grid of hexa-ferrocene assembly [*n*-BuSn(O)OC(O)CH$_2$C$_5$H$_4$-Fe-C$_5$H$_5$]$_6$

[#] *Rangoli is a repetitive decorative pattern drawn in front of many homes in India during festive seasons*
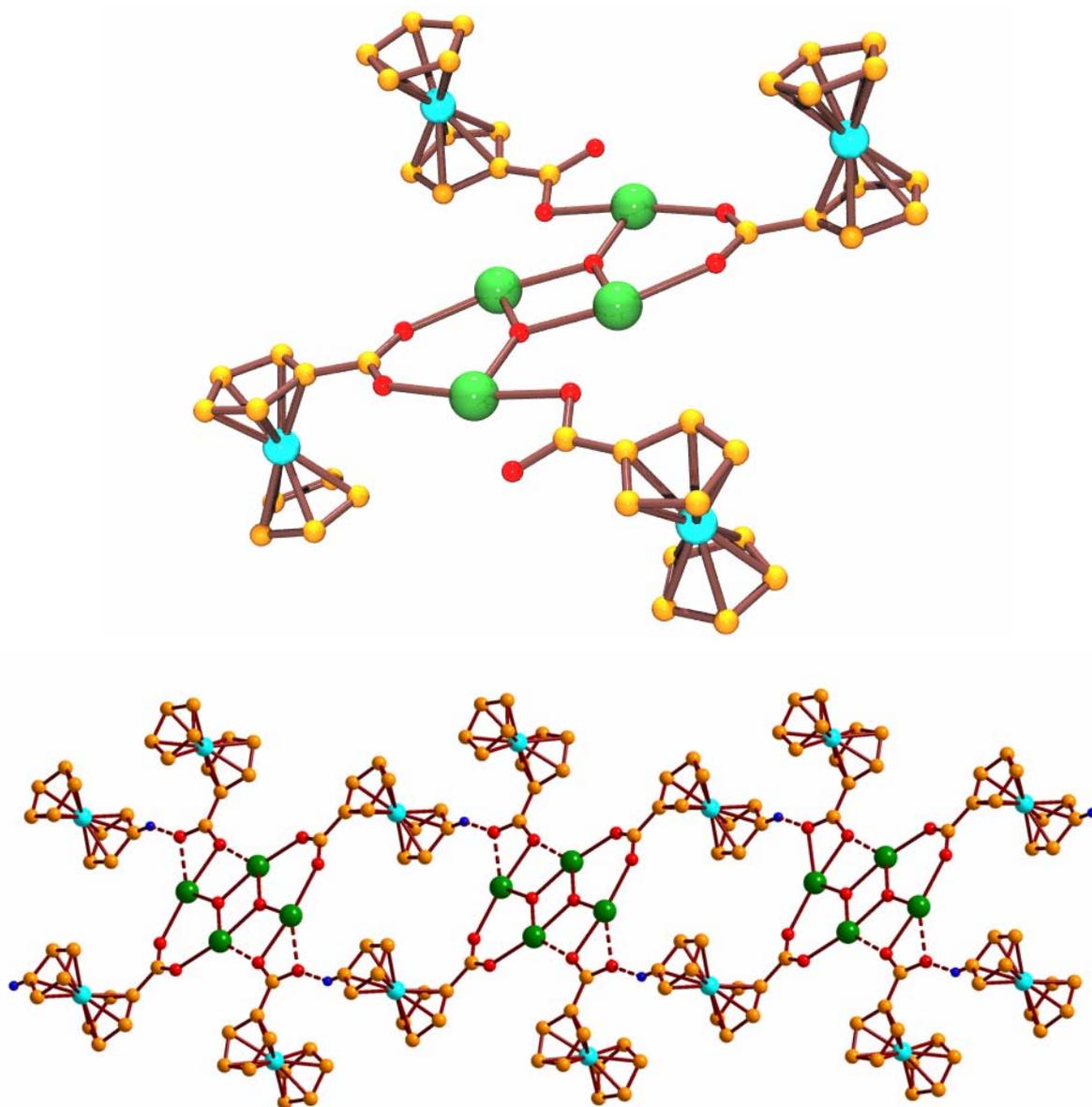
Figure 6. Molecular and staircase like 1D-polymeric chain (due to C-H---O interactions) of the tetra-ferrocene assembly, {[n-Bu$_2$SnOC(O)C$_5$H$_4$-Fe-C$_5$H$_5$]$_2$O}$_2$
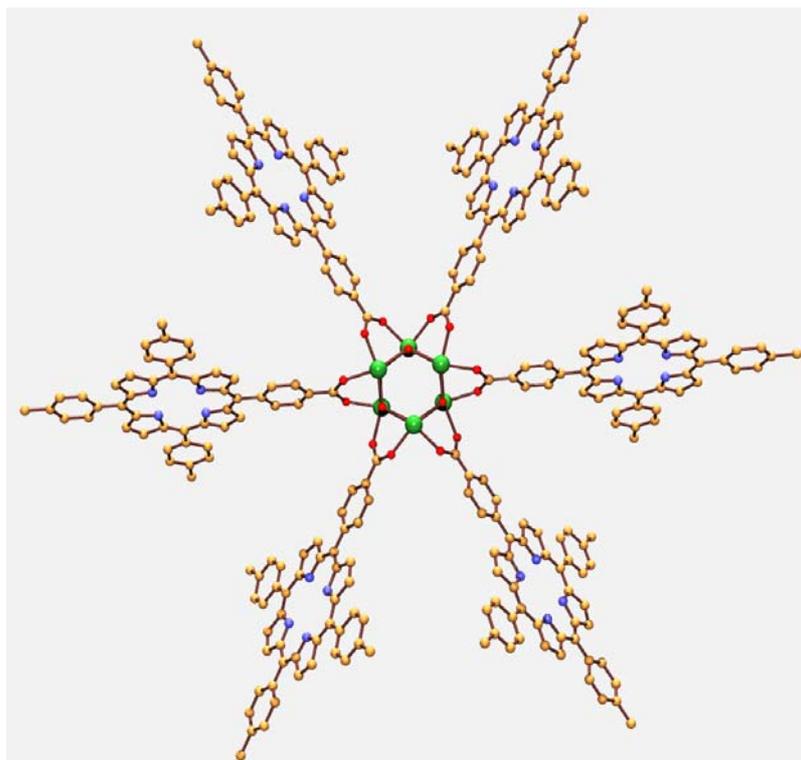
Figure 7. A structural model for the hexa-porphyrin assembly,
[n-BuSn(O)OC(O)H$_2$TTP]$_6$ (not to scale)
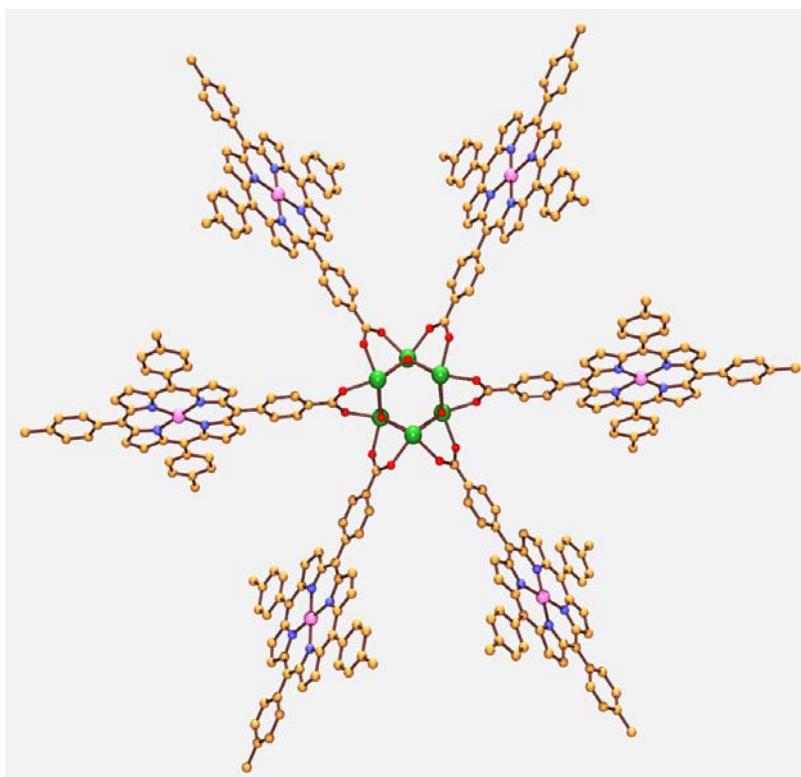
Figure 8. A structural model for the hexa-Cu(II)porphyrin assembly,
[n-BuSn(O)OC(O)CuTTP]$_6$ (not to scale)
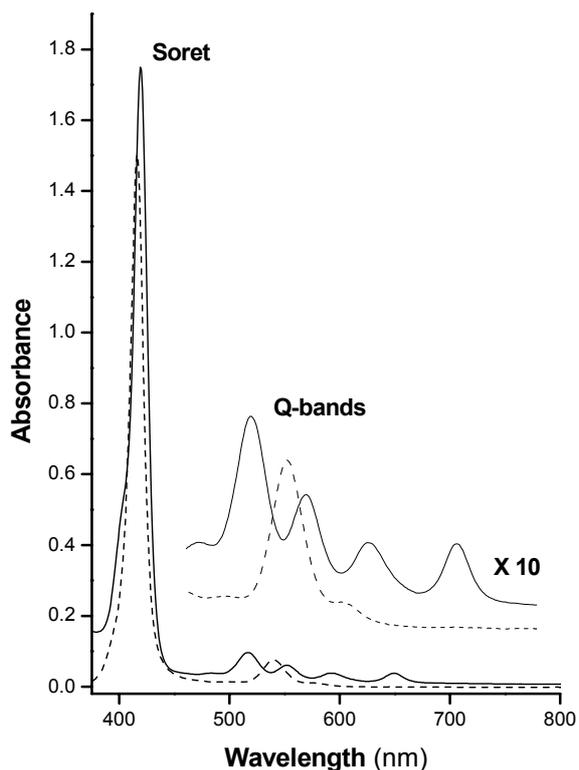
Figure 9. Electronic absorption spectrum of the hexa-porphyrin (———) and hexa-Cu(II)porphyrin (-----) assemblies (in 1 x 10^{-6} M dicloromethane solution)

Magnetic Field (Gauss)
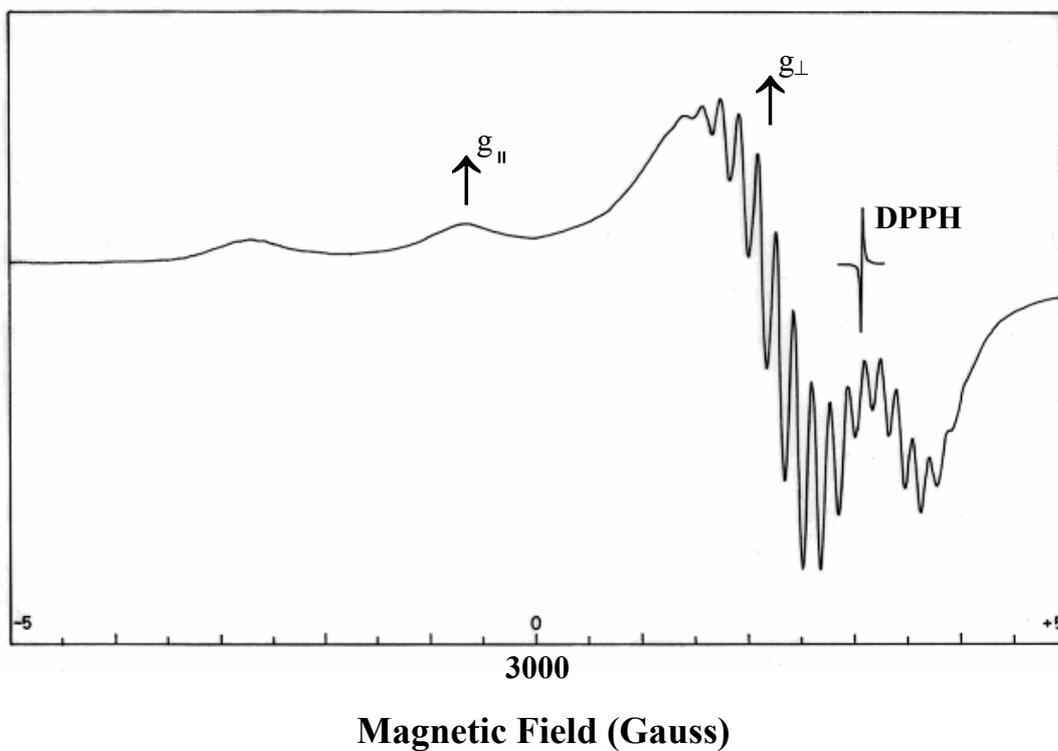
Figure 10. EPR spectrum of the hexa-Cu(II)porphyrin assembly [*n*-BuSn(O)OC(O)CuTTP]$_6$, at liquid nitrogen temperature
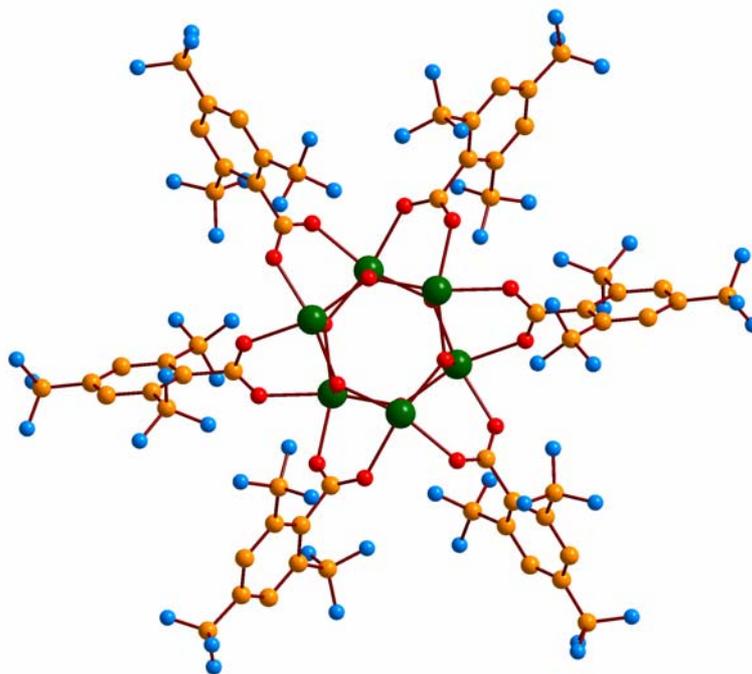
Figure 11. X-ray crystal structure of the fluorine mammoth, [*n*-BuSn(O)OC(O)(2,4,6-(CF$_3$)$_3$C$_6$H$_2$)]$_6$ which contains 54 fluorine atoms in its periphery
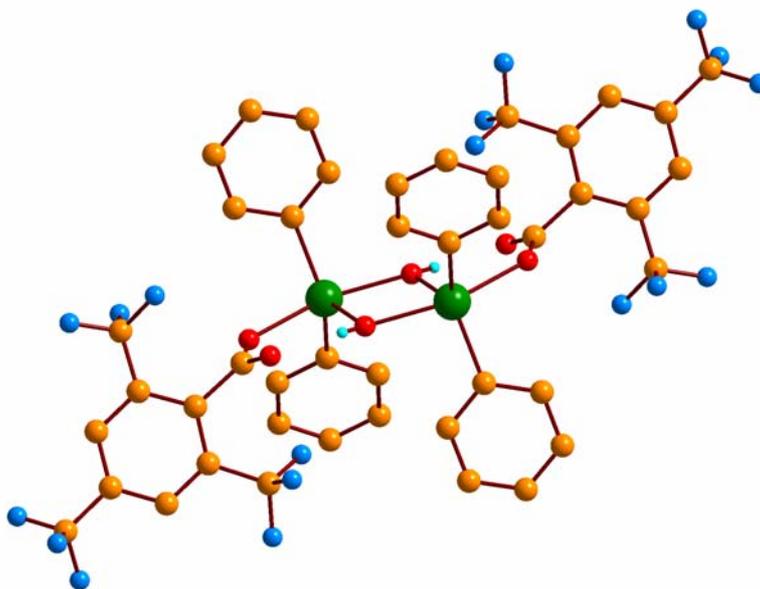
Figure 12. X-ray crystal structure of the Sn-C bond cleaved product [Ph$_2$Sn(OH)OC(O)(R$_f$)]$_2$
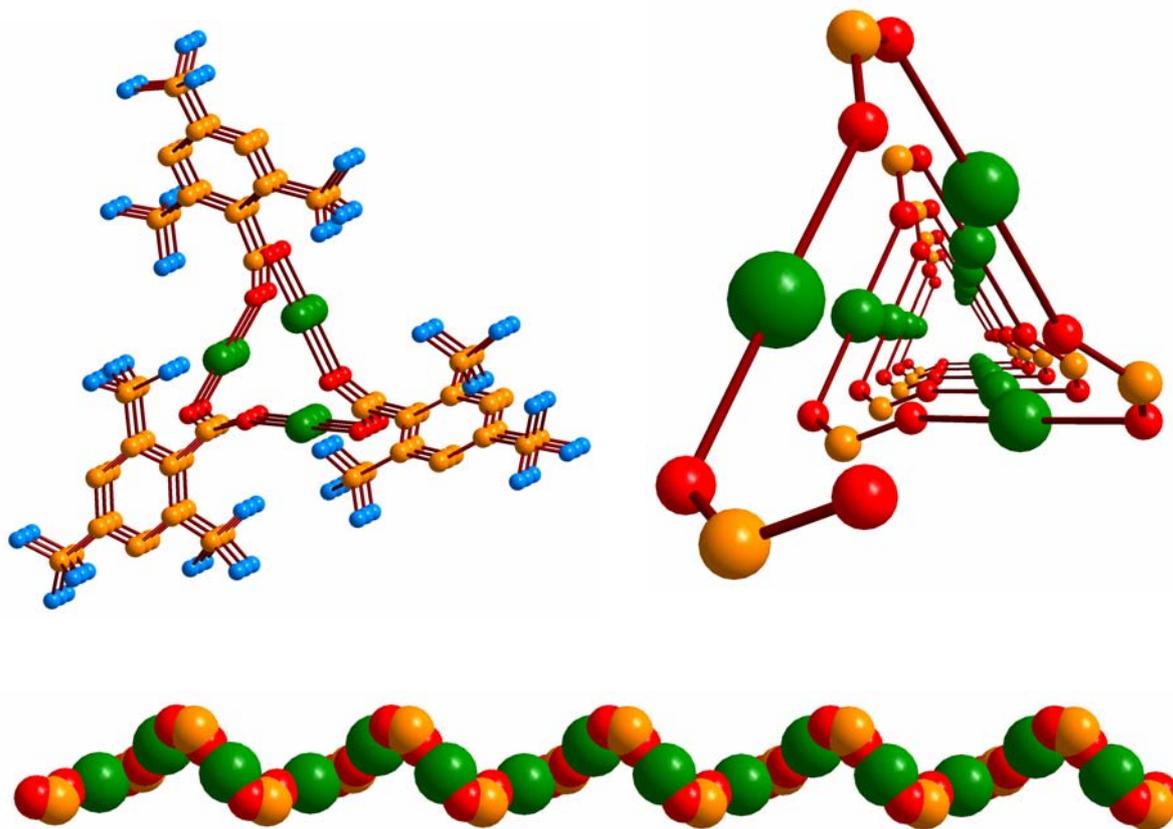
Figure 13. X-ray crystal structure of the 1D-helical coordination polymer, [*n*-Bu₃OC(O)R$_f$]$_n$. Also shown are its helicity in two different views
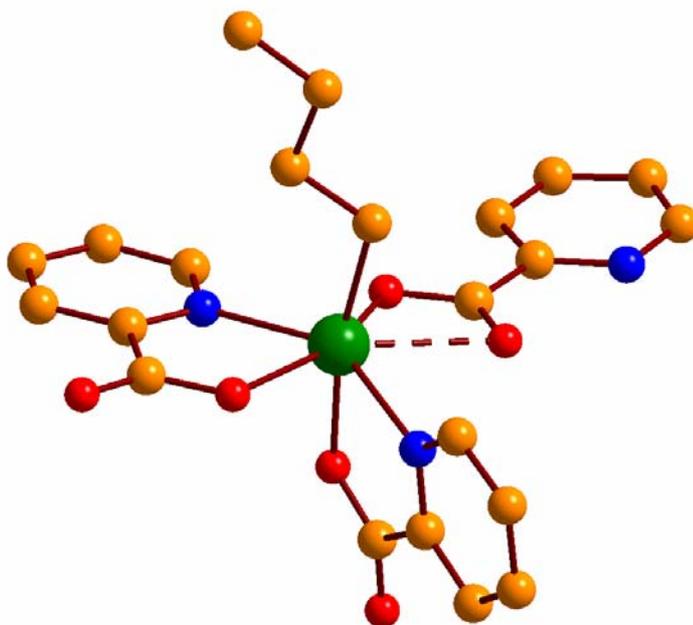

Figure 14. X-ray crystal structure of the first monoorganotin tricarboxylate, *n*-BuSn(O₂CC₅H₄N)₃

(a)

(b)
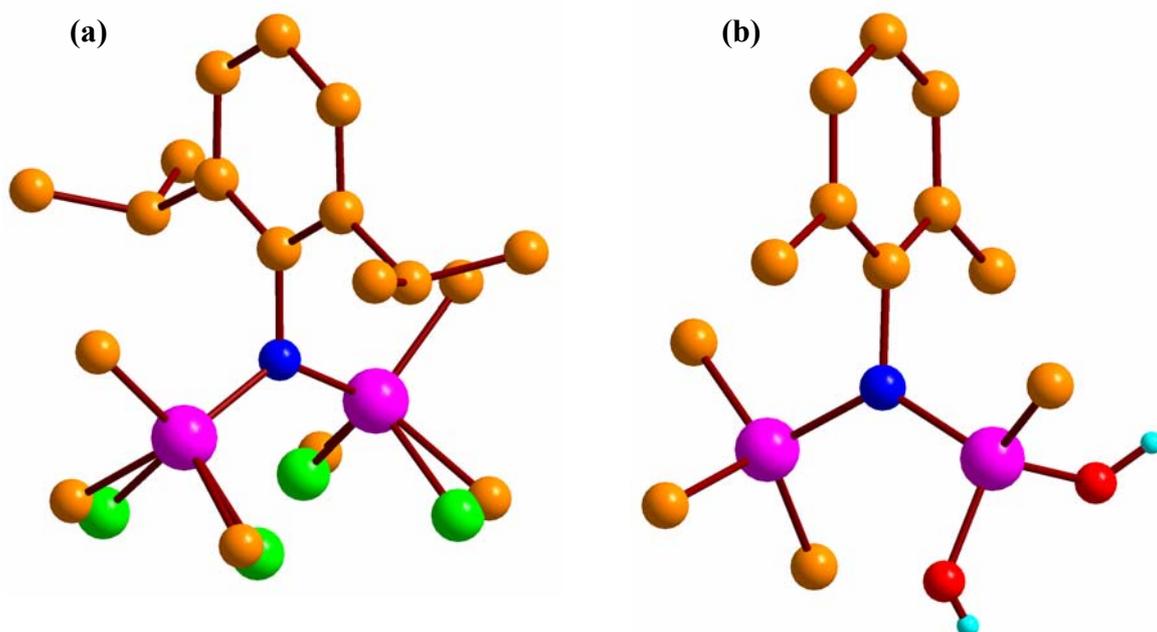
Figure 15. X-ray crystal structure of (a) the N-bonded silicon dichloride [2,6-*i*-Pr$_2$C$_6$H$_3$N (SiMe$_3$)(SiMeCl$_2$)] and (b) the N-bonded silicon diol [2,6-Me$_2$C$_6$H$_3$N(SiMe$_3$)(SiMe(OH)$_2$)]

(a)

(b)
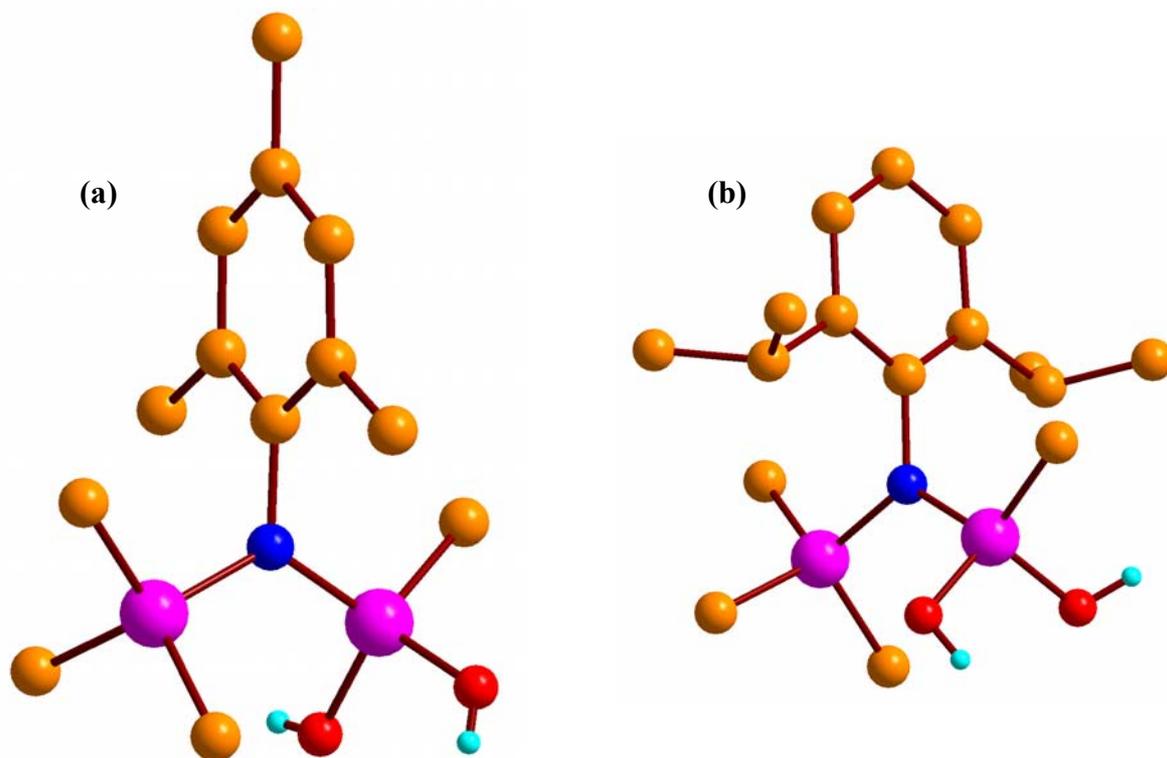
Figure 16. X-ray crystal structure of the N-bonded silicon diols (a) [2,4,6-Me$_3$C$_6$H$_2$N(SiMe$_3$)(SiMe(OH)$_2$)] and (b) [2,6-*i*-Pr$_2$C$_6$H$_3$N(SiMe$_3$)(SiMe(OH)$_2$)]
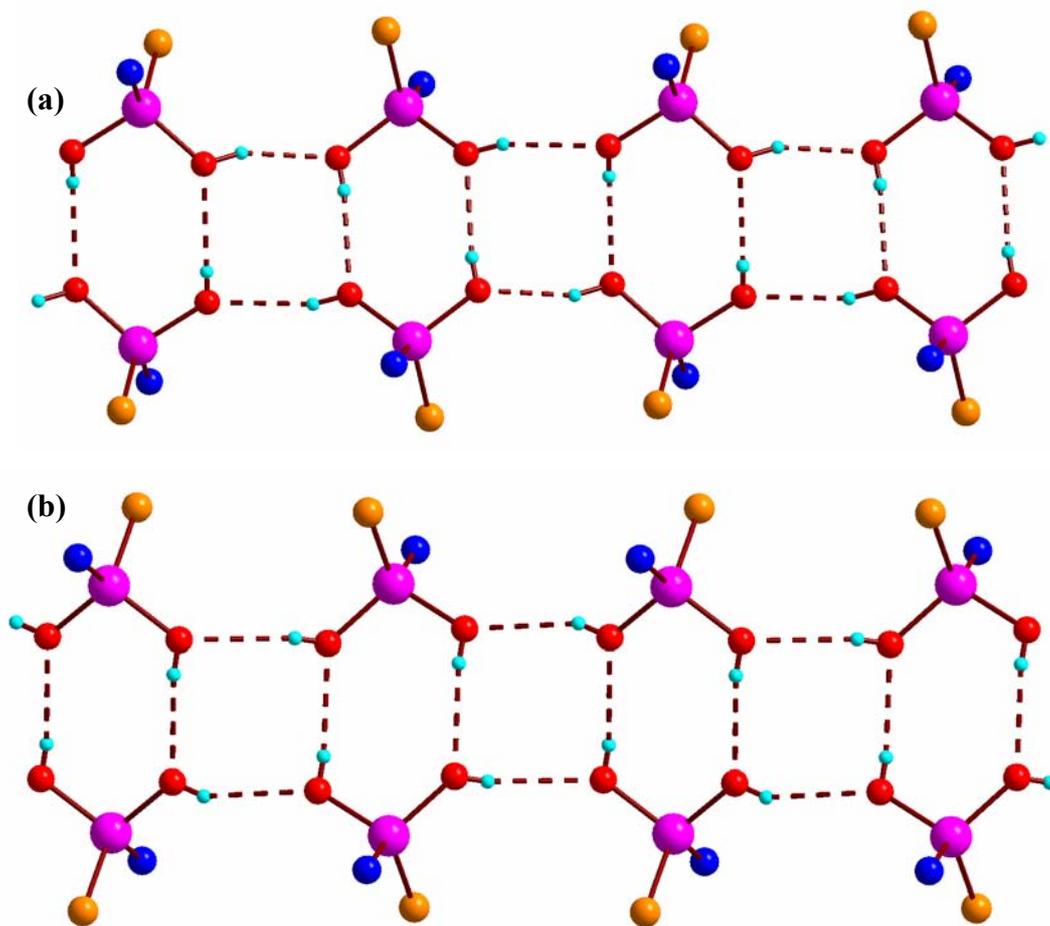
Figure 17. 1D-polymeric ribbons in the solid-state structures of (a) xylyl and (b) mesityl diols due to strong O-H---O hydrogen bonding
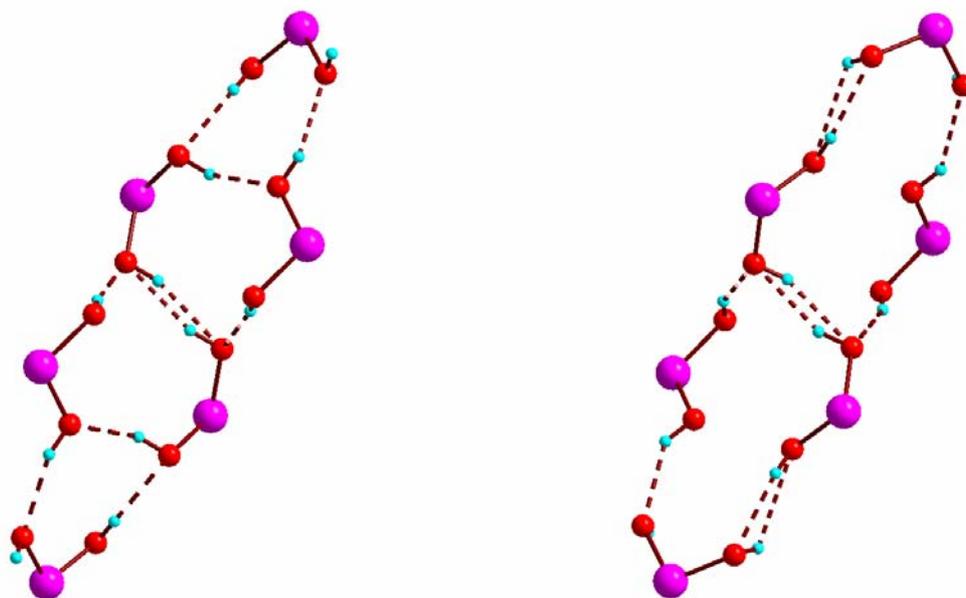

Figure 18. Discrete hexameric clusters in the solid-state structure of isopropyl diol due to strong O-H---O hydrogen bonding
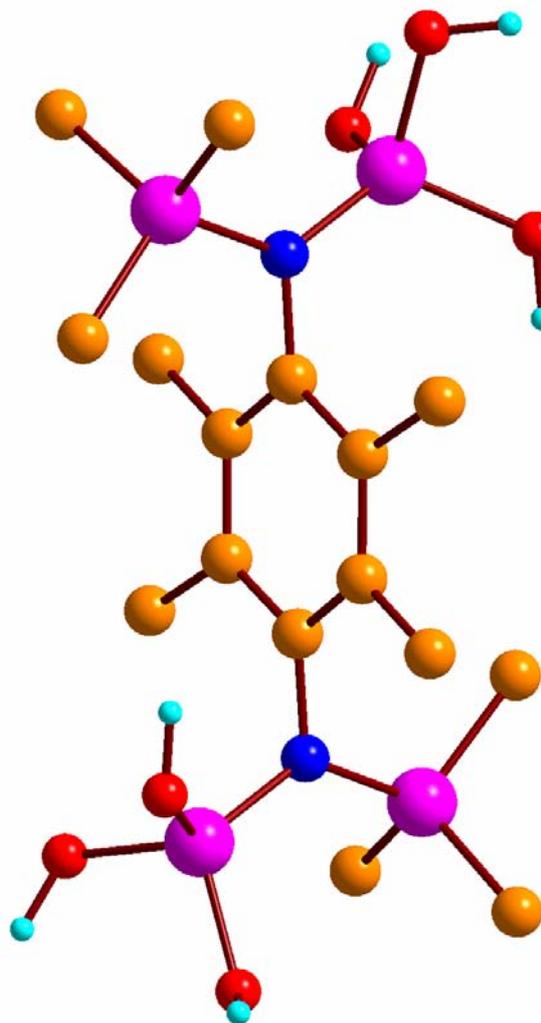
Figure 19. Energy minimized structure of the bis-N-bonded silanetriol [(OH)$_3$SiN(SiMe$_3$)]$_2$C$_6$(2,3,5,6-Me$_4$) obtained from semi-empirical AM1 calculation